8-2013

Mimicry epitope from *Ehrlichia canis* for interphotoreceptor retinoid-binding protein 201–216 prevents autoimmune uveoretinitis by acting as altered peptide ligand

Arunakumar Gangaplara
University of Nebraska-Lincoln

Chandirasegaran Massilamany
University of Nebraska-Lincoln, cmassilamany@unl.edu

David Steffen
University of Nebraska-Lincoln, dsteffen1@unl.edu

Jay Reddy
University of Nebraska-Lincoln, jayreddy@unl.edu

Published in *Journal of Neuroimmunology* 263: 1–2 (2013), pp. 98–107; doi: 10.1016/j.jneuroim.2013.08.006

Submitted December 17, 2012; revised May 28, 2013; accepted August 12, 2013; published online August 17, 2013.

Mimicry epitope from *Ehrlichia canis* for interphotoreceptor retinoid-binding protein 201–216 prevents autoimmune uveoretinitis by acting as altered peptide ligand

Arunakumar Gangaplara, Chandirasegaran Massilamany, David Steffen, and Jay Reddy

School of Veterinary Medicine and Biomedical Sciences, University of Nebraska–Lincoln, Lincoln, NE 68583

Corresponding author — J. Reddy, Room 202, Bldg. VBS, School of Veterinary Medicine and Biomedical Sciences, University of Nebraska-Lincoln, Lincoln, NE 68583; tel 402 472-8541, fax 402 472-9690, email nreddy2@unl.edu

Abstract

We report here identification of novel mimicry epitopes for interphotoreceptor retinoid-binding protein (IRBP) 201–216, a candidate ocular antigen that causes experimental autoimmune uveoretinitis (EAU) in A/J mice. One mimicry epitope from *Ehrlichia canis* (EHC), designated EHC 44–59, induced cross-reactive T cells for IRBP 201–216 capable of producing T helper (Th)1 and Th17 cytokines, but failed to induce EAU in A/J mice. In addition, animals first primed with suboptimal doses of IRBP 201–216 and subsequently immunized with EHC 44–59 did not develop EAU; rather, the mimicry epitope prevented the disease induced by IRBP 201–216. However, alteration in the composition of EHC 44–59 by substituting alanine with valine at position 49, similar to the composition of IRBP 201–216, enabled the mimicry epitope to acquire uveitogenicity. The data provide new insights as to how microbes containing mimicry sequences for retinal antigens can prevent ocular inflammation by acting as naturally occurring altered peptide ligands.

Keywords: Autoimmunity, Experimental autoimmune uveoretinitis, Molecular mimicry, Interphotoreceptor retinoid-binding protein, Cross-reactive T cells

Abbreviations: 7-AAD, 7-aminoactinomycin D; APL, altered peptide ligand; CFA, complete Freund's adjuvant; CLIP, class-II associated invariant chain peptide; CLN, *Clostridium novyi*; cpm, counts per minute; CTR, *Chlamydia trachomatis*; DELFIA, dissociation-enhanced lanthanide fluoroimmunoassay; EAU, experimental autoimmune uveoretinitis; EHC, *Ehrlichia canis*; HEC, hepatitis C virus; HEL, hen egg white lysozyme; IRBP, interphotoreceptor retinoid-binding protein; IL, interleukin; IC_{50}, half maximal inhibitory concentration; IFN, interferon; LN, lymph nodes; LNC, lymph node cells; MHC, major histocompatibility complex; PAB, *Paracoccidioides brasiliensis*; PMA, phorbol 12-myristate 13-acetate; PSP, *Pseudomonas putida*; PT, pertussis toxin; RNase, bovine ribonuclease; RT, room temperature; SA, streptavidin; TCR, T cell receptor; tet^+, tetramer positive; TRC, *Trypanosoma cruzi*.

1. Introduction

The eye is generally considered an immunologically privileged organ, and several mechanisms have been postulated to explain this phenomenon (Streilein et al., 2002; Caspi, 2006; Vallochi et al., 2007; Benhar et al., 2012). These include sequestration of antigens behind the blood–retinal barrier; lack of lymphatic drainage; absence of professional antigen-presenting cells; and the existence of an inherently bestowed immune-suppressive environment through the production of cytokines like transforming growth factor-β (Cousins et al., 1991; Hamrah and Dana, 2007; Forrester and Xu, 2012). Because of sequestration, ocular antigens are not expected to be recognized by the developing thymocytes, leading to their escape from central tolerance. However, this notion is increasingly being challenged, following demonstration of the expression of various retinal antigens, like interphotoreceptor retinoid-binding protein (IRBP), and soluble antigens within the thymus (Charukamnoetkanok et al., 1998; Takase et al., 2005). Nonetheless, alterations in the amounts of protein expression can still affect thymic education of T cells, leading to their safe exit into the peripheral repertoires (Anderson et al., 2000; Klein et al., 2000). In genetically susceptible individuals, such a pre-existing repertoire of self-reactive T cells can be activated to become pathogenic cells, as might occur in response to exposure to infectious agents. This phenomenon may involve a combination of mechanisms, such as bystander activation, release of cryptic epitopes, epitope spreading and molecular mimicry (Miller et al., 1997b; Oldstone, 2005; Fujinami et al., 2006).

Molecular mimicry is a natural phenomenon in which microbes carrying sequences identical to those found in self-antigens can lead to the generation of cross-reactive immune responses directed against both foreign and self-antigens (Fujinami and Oldstone, 1985; Fujinami et al., 2006). Several experimental examples provide a proof-of-concept that the microbial mimics can break self-tolerance and induce autoimmunity (Miller et al., 1997b; Oldstone, 2005; Fujinami et al., 2006). Conversely, pathogens that primarily affect the target organs can lead to secondary generation of autoimmune responses by epitope spreading, as shown with Theiler's murine encephalomyelitis virus-induced demyelination model in SJL mice (Miller et al., 1997a; Olson et al., 2002). However, when a disease process involves both molecular mimicry and epitope spreading, the former generally precedes the latter.

Our studies involve IRBP 201–216-induced experimental autoimmune uveoretinitis (EAU) in A/J mice. Using IRBP 201–216 as a putative ocular antigen (Namba et al., 1998; Agarwal et al., 2012), we searched for mimicry sequences from pathogens primarily affecting the eyes, with an expectation that such microbes can serve as ideal candidates to delineate autoimmune events in the immune pathogenesis of eye diseases. This search resulted in the identification of 48 novel sequences belonging to various classes of microbes. One of these mimicry epitopes, derived from *Ehrlichia canis* (EHC) and designated EHC 44–59, induces cross-reactive T cells for IRBP 201–216 capable of producing inflammatory cytokines of T helper (Th)1 and Th17 subsets. Unexpectedly, EHC 44–59 failed to induce EAU; rather, it prevented the development of disease induced by IRBP 201–216, possibly by acting as a naturally occurring altered peptide ligand (APL).

2. Materials and methods

2.1. Mice

Six- to eight-week-old female, A/J mice carrying the H-2^a allele IA^k at the major histocompatibility complex (MHC) class II locus were procured from Jackson Laboratory (Bar Harbor, ME). The animals were maintained in accordance with the animal protocol guidelines of the University of Nebraska-Lincoln, Lincoln, NE.

2.2. Identification of mimicry epitopes for IRBP 201–216

We used bovine IRBP 201–216 (ADKDVVVLTSSRTGGV) as a disease-inducing retinal antigen (Caspi, 2003), in which the putative MHC class II- and T cell receptor (TCR)-binding sites have been identified (Figure 1; Namba et al., 1998). Using this sequence, we performed pattern searches using the prosite scan of the Bioinformatics Toolkit (http://toolkit.tuebingen.mpg.de/patsearch, Max-Planck Institute for Developmental Biology, Tuebingen, Germany). The pattern used was X**D**XDXXXXX**S**XXXXXX (underlined: TCR-contact residue; bold: MHC-anchor residues; X: non-critical residues).

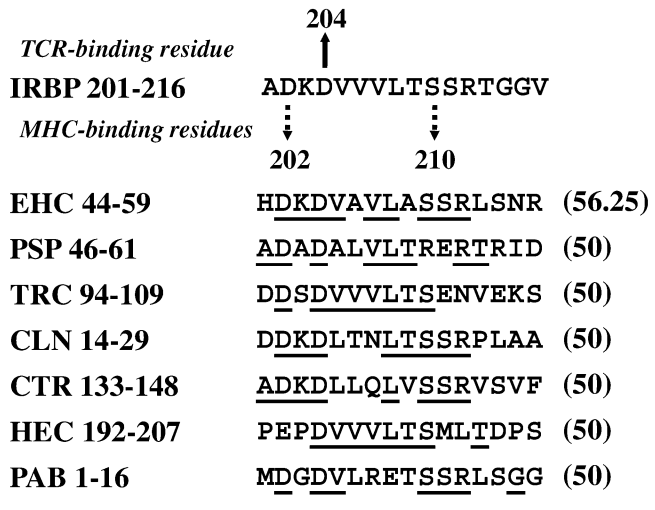

Figure 1. Comparison of microbial peptide sequences with IRBP 201–216. The peptide sequence of IRBP 201–216 was compared with the mimicry epitopes derived from various microbes. IRBP, Interphotoreceptor retinoid-binding protein; EHC, *Ehrlichia canis*; PSP, *Pseudomonas putida*; TRC, *Trypanosoma cruzi*; CLN, *Clostridium novyi*; CTR, *Chlamydia trachomatis*; HEC, hepatitis C virus; PAB, *Paracoccidoides brasiliensis*. Putative TCR- and MHC-binding residues are shown, respectively, with top and bottom arrows. Identical residues are underlined, and the numbers in parentheses indicate the percent sequence identities with IRBP 201–216.

2.3. Peptide synthesis

Peptides synthesized commercially on 9-fluorenylmethyloxycarbonyl chemistry (Neopeptide, Cambridge, MA) include IRBP 201–216; EHC 44–59, HDKDVAVLASSRLSNR; *Pseudomonas putida* (PSP) 46–61, ADADALVLTRERTRID; *Trypanosoma cruzi* (TRC) 94–109, DDSDVVVLTSENVEKS; *Clostridium novyi* (CLN) 14–29, DDKDLTNLTSSRPLAA; *Chlamydia trachomatis* (CTR) 133–148, ADKDLLQLVSSRVSVF; hepatitis C virus (HEC) 192–207, PEPDVVVLTSMLTDPS; *Paracoccidioides brasiliensis* (PAB) 1–16, MDGDVLRETSSRLSGG; bovine ribonuclease (RNase) 43–56, VNTFVHESLADVQA; N-terminal biotinylated hen egg white lysozyme (HEL) 46–61, YNTDGSTDYGILQINSR; and three APLs, designated with subscript 'AP' and a number 1, 2 or 3: EHC 44–59$_{AP1}$, HDKDVVVLASSRLSNR; EHC 44–59$_{AP2}$, HDKDVAVLTSSRLSNR and EHC 44–59$_{AP3}$, HDKDVVVLTSSRLSNR. All peptides were HPLC-purified (> 90%), confirmed by mass spectroscopy and dissolved in sterile 1 × PBS prior to use.

2.4. Immunization procedures

To measure recall responses, peptides were emulsified in complete Freund's adjuvant (CFA) and administered s.c. (50 μg/mouse) in the inguinal and sternal regions and foot-pads (Massilamany et al., 2011a, 2011b). For disease induction, peptides were emulsified in CFA supplemented with *Mycobacterium tuberculosis* H37RA extract (Difco Laboratories, Detroit, MI) to a final concentration of 5 mg/ml, and the emulsions were administered at indicated doses s.c. in the inguinal and sternal regions and base of the tail. Additionally, pertussis toxin (PT; List Biological Laboratories, Campbell, CA) was administered i.p. at indicated doses on day 0 and day 2 postimmunization (Silver et al., 1995; Namba et al., 1998).

2.5. T cell proliferation assay

Groups of A/J mice were immunized with the indicated peptides, and at termination on day 10 or day 21, the animals were euthanized, and the draining lymph nodes (LN) were harvested to prepare single cell suspensions (Massilamany et al., 2011b). Lymph node cells (LNC) were stimulated with the indicated peptides (0–100 μg/ml) at a density of 5 × 10^6 cells/ml for two days in growth medium containing 1 × RPMI medium supplemented with 10% fetal bovine serum, 1 mM sodium pyruvate, 4 mM l-glutamine, 1 × each of non-essential amino acids and vitamin mixture, and 100 U/ml penicillin–streptomycin (Lonza, Walkersville, MD). Cultures were then pulsed with 1 μCi of tritiated ^{3}[H] thymidine/well (MP Biomedicals, Santa Ana, CA); 16 h later, the proliferative responses were measured as counts per minute (cpm) using a Wallac liquid scintillation counter (PerkinElmer, Waltham, MA; Massilamany et al., 2011a; Gangaplara et al., 2012).

2.6. IA^k-binding assay

To determine the affinities of peptides binding to IA^k, we used soluble IA^k molecules expressed in baculovirus as we have described previously (Massilamany et al., 2011a, 2011b). Briefly, IA^k constructs representing the extracellular domains of IA^k-α and IA^k-β were designed, in which the sequence of class II-associated invariant-chain peptide (CLIP) 88–102 (VSQMRMATPLLMRPM) was tethered into the N-terminus of the IA^k-β construct, followed by introduction of a thrombin cleavage site to facilitate the release of the CLIP peptide. Soluble IA^k molecules were expressed in baculovirus using sf9 insect cells, purified on an anti-IA^k affinity column (clone, 10–2.16; BioXcell, West Lebanon, NH) and cleaved with thrombin to obtain empty IA^k molecules (Day et al., 2003; Massilamany et al., 2011b). Cocktails of individual reaction mixtures were prepared to include thrombin-cleaved IA^k monomers (0.35 μg), competitor peptides [IRBP 201–216 or EHC 44–59 (0.000005 μM to 50 μM)] or al-

tered peptides of EHC 44–59 (0.00001 μM to 100 μM), and a constant amount of biotinylated reference peptide, HEL 46–61 (1 μM), in a buffer containing 50 mM sodium phosphate pH 7.0, 100 mM sodium chloride, 1 mM EDTA, and 1 × protease inhibitor (Sigma-Aldrich, St. Louis, MO; Hausmann et al., 1999; Massilamany et al., 2011b). The mixtures were incubated at room temperature (RT) overnight. In parallel, anti-IA^k (10 μg/ml) was coated onto 96-well white fluorescence plates (Nunc, Rochester, NY) in sodium phosphate buffer 0.2 M, pH 6.8 overnight. Plates were washed five times with 1 × wash buffer (PerkinElmer) and blocked with 2% casein for 2 h at 37 °C. After washing, the reaction mixtures described above were added in duplicate for each peptide and incubated on a rocker at RT for 1 h and washed. Europium-labeled streptavidin (SA) was then added to a concentration of 1 μg/ml in dissociation-enhanced lanthanide fluoroimmunoassay (DELFIA) buffer, followed by DELFIA-enhancement solution (PerkinElmer). Fluorescence intensities were measured at excitation/emission wavelengths of 340/615 nm using a Victor Multi Label Plate Reader (PerkinElmer). Concentrations of competitor peptides that prevented 50% binding of the reference peptide (HEL 46–61) were taken as the half maximal inhibitory concentration (IC_{50}) for each peptide (Hausmann et al., 1999; Massilamany et al., 2011b).

2.7. Enumeration of the frequencies of antigen-specific CD4 T cells by MHC class II/IA^k tetramer staining

To determine the frequency of antigen-specific cells, LNC were obtained from mice immunized with IRBP 201–216 or EHC 44–59, and the cells were stimulated with the indicated peptides (50 μg/ml) for two days and maintained in growth medium containing interleukin (IL)-2 (eBioscience, San Diego, CA; Advanced Biotechnologies, Columbia, MD). Viable lymphoblasts were harvested on day 5 by Ficoll-Hypaque density gradient centrifugation, washed twice using 1 × PBS to remove antigens; the cultures then were maintained in growth medium containing IL-2. On day 9, cells were stained with IA^k/tetramers, anti-CD4 (eBioscience), and 7-aminoactinomycin D (7-AAD; Invitrogen, Carlsbad, CA) as we have previously described (Massilamany et al., 2010, 2011a). After acquiring the cells by flow cytometry (FACSCalibur, BD Biosciences, San Diego, CA), percentages of tetramer positive (tet^+) cells were determined in the live (7-AAD^-) $CD4^+$ subset using FlowJo software (Tree Star, Ashland, OR).

2.8. Intracellular cytokine staining

Groups of mice were immunized with the indicated peptides. At termination, draining LNs were harvested to prepare single-cell suspensions. Cells were stimulated with the corresponding peptides (50 μg/ml) for two days and maintained in growth medium containing IL-2. On day 5 poststimulation, viable lymphoblasts were harvested by Ficoll-Hypaque density gradient centrifugation and washed twice using 1 × PBS to remove antigen. Cells were then stimulated with phorbol 12-myristate-13 acetate (PMA, 10 ng/ml) and ionomycin (150 ng/ml; Sigma-Aldrich) for five hours in the presence of 2 mM monensin (GolgiStop, BD Pharmingen, San Diego, CA; Gangaplara et al., 2012; Massilamany et al., 2009). After staining with anti-CD4 and 7-AAD, cells were fixed, permeabilized and stained with anti-cytokine antibodies along with their respective isotype controls (eBioscience). The cells were then acquired by flow cytometry, and the frequencies of cytokine-producing cells were determined in the live (7-AAD^-) $CD4^+$ subset. The clones of cytokine antibodies used were: IL-2 (JES6-5H4); interferon (IFN)-γ (XMG1.2); IL-4 (11B11); IL-10 (JES5-16E3); IL-17A (eBio 17B7); and IL-17 F (eBio 18F10) (all from eBioscience).

2.9. Histopathology

At termination, the animals were euthanized and eyes were harvested. The freshly enucleated eyes were fixed in Davidson's stock solution containing 10% phosphate-buffered formalin and 90% ethanol (Fisher Scientific, Pittsburgh, PA), and the eyes were cross-sectioned at a thickness of 5 μm and stained by hematoxylin and eosin (H and E) staining (Silver et al., 1995; Namba et al., 1998). Eyes were evaluated for inflammation by counting the foci in both eyes corresponding to the corneal–scleral junction, iris, cornea, choroid and retina; the counts were then added. Based on the morphology of infiltrating cells, inflammation was classified as neutrophilic, lymphocytic or mixed.

Table 1. Peptide sequences that mimic IRBP 201–216.

Source	Sequence[a]	Identity (%)
IRBP 201–216	ADKDVVVLTSSRTGGV	
Bacteria		
Brevibacterium linens BL2	ADKDVKWLTRERTTGT	62.5
Ehrlichia canis str. Jake	HDKDVAVLASSRLSNR	56.25
Catenulispora acidiphila DSM 44928	PDGDVVVLTSKDFEGL	56.25
Shewanella halifaxensis HAW-EB4	ADIARKALTSSRTIIV	56.25
Pyrococcus horikoshii OT3	ADLDVVIATSRRGVDV	56.25
Clostridium novyi NT	DDKDLTNLTSSRPLAA	50
Chlamydia trachomatis 434/Bu	ADKDLLQLVSSRVSVF	50
Pseudomonas aeruginosa UCBPP-PA14	KDYDVVYATSSRLMTA	50
Burkholderia phytofirmans PsJN	ADVDVSPLTSERAMAL	50
Vibrio parahaemolyticus 16	EDYDVVFATSSRLFTA	50
Salmonella enterica subsp. *enterica* serovar *Typhi* str. CT18	KGADVVVLTSGQTENK	50
Metallosphaera sedula DSM 5348	CSVDVVVLTSSLIAKS	50
Citrobacter koseri ATCC BAA-895	KGADVVVLTSGQTDNK	50
Salmonella enterica subsp. *enterica* serovar *Typhi* str. E02-1180	KGADVVVLTSGQTENK	50
Salmonella enterica subsp. *enterica* serovar *Paratyphi C* strain RKS4594	KGADVVVLTSGQTENK	50
Citrobacter sp. 30_2	KGADVVVLTSGQTDNK	50
Citrobacter youngae ATCC 29220	KGADVVVLTSGQTDNK	50
Pseudomonas putida KT2440	ADADALVLTRERTRID	50
Mycobacterium smegmatis str. MC2 155	ADGDDHRLTGSRTLVS	50
Burkholderia pseudomallei 9	ADGAIGVLTLSRTQDP	50
Helicobacter bilis ATCC 43879	RDKDAYNLISSRLKPI	43.75
Pseudomonas syringae pv. *syringae* B728a	PDVDVSLVTSERTHSM	43.75
Rhodopseudomonas palustris TIE-1	ADPDVLRMTSLRAHDQ	43.75
Rhodopseudomonas palustris HaA2	DARDVVVLTSRPAQLS	43.75
Rhodococcus jostii RHA1	NIMDVVVLTSVLSCLN	43.75
Cyanobium sp. PCC 7001	NHADVVVLTSPAQYPA	43.75
Acidobacterium capsulatum ATCC 51196	EGSDVVVLTSDNPRSE	43.75
Rhodococcus erythropolis PR4	NIMDVVVLTSVLSCLN	43.75
Rhodococcus opacus B4	NIMDVVVLTSVLSCLN	43.75
Kingella kingae	ADADLSELTIERTAQG	43.75
Fungi		
Schizosaccharomyces japonicus yFS275	DDKDFSVLHSSRLRSM	50
Paracoccidioides brasiliensis Pb18	MDGDVLRETSSRLSGG	50
Aspergillus niger	KDKDGNYLLSSRHFST	43.75
Magnaporthe grisea 70-15	GDDDVFVDTSTRSPLP	43.75
Sclerotinia sclerotiorum 1980	DDEDVEFFTSKQRKV	43.75
Malassezia globosa CBS 7966	LDVDVPIETSERTAFT	43.75
Ajellomyces capsulatus NAm1	ADKDLNINKSSRPSKA	43.75
Algae		
Ostreococcus lucimarinus CCE9901	ADGKSVDLTISRTGED	56.25
Chlamydomonas reinhardtii	FDKDMQELTSSRRILD	50
Phaeodactylum tricornutum CCAP 1055/1	ADEDAVGLTQRRTTTA	50
Guillardia theta	ADPELLKLTSDRTLFE	43.75
Protozoa		
Dictyostelium discoideum AX4	ADKKNSTLTSSRGNNK	50
Trypanosoma cruzi strain CL Brener	DDSDVVVLTSENVEKS	50
Leishmania braziliensis MHOM/BR/75/M2904	ADKDDPLALSSRSPML	43.75
Viruses		
Hepatitis C virus	PEPDVVVLTSMLTDPS	50
Helminths		
Brugia malayi	SDSDVEAATSSRKRKT	43.75
Others		
Strongylocentrotus purpuratus (sea urchin)	IDLDVVVLTSSGNDRR	56.25
Trichoplax adhaerens (metazoan)	EDKDNQLLASSRRFAQ	43.75

a. Identical residues are underlined.

2.10. Statistics

Differences in T cell proliferative responses, IA^k-binding affinities and cytokine analysis were determined using Student's t-test. $p \leq 0.05$ values were considered significant. Stimulation indices indicated as 'fold increase' were calculated using the following formula: cpm values obtained in peptide-stimulated cultures / cpm values obtained in medium control.

3. Results

3.1. Identification of mimicry epitopes for IRBP 201–216

IRBP is recognized as one of the candidate retinal antigens in EAU pathogenesis (Agarwal et al., 2012), and we used IRBP 201–216 to identify mimicry sequences for two reasons: 1) IRBP 201–216 induces EAU in susceptible mouse strains like A/J mice by generating IRBP-reactive T cells (Caspi, 2003); and 2) its putative MHC class II (IA^k)- and TCR-contact residues have been identified (Namba et al., 1998). While aspartic acid (Asp) at position 202 and serine (Ser) at 210 are predicted to anchor the IA^k molecule, Asp at position 204 is supposedly a TCR-contact residue (Figure 1; Namba et al., 1998). In our search, we kept these residues constant, with an expectation that the mimicry epitopes bearing the critical MHC- and TCR-contact residues should be able to induce cross-reactive T cell responses for IRBP 201–216. This analysis led us to identify 48 sequences – belonging to various microbes such as bacteria, viruses, fungi, algae, protozoa and helminths, including two marine organisms – that show a similarity of 43.75 to 62.5% with IRBP 201–216 (Table 1). We chose a panel of seven of these mimics from microbes that have been implicated in various eye diseases for further testing (Figure 1). All the epitopes, except the viral mimic HEC 192–207, contained both MHC- and TCR-contact residues, making them ideal candidates to test for their immunogenicity.

3.2. T cells sensitized with IRBP 201–216 and EHC 44–59 cross-react with each peptide

Using T cell proliferation assay based on ^{3}[H] thymidine incorporation, we first verified whether IRBP-reactive T cells can respond to mimicry epitopes by cross-reactivity. Briefly, LNC were isolated from mice immunized with IRBP 201–216, and the re-

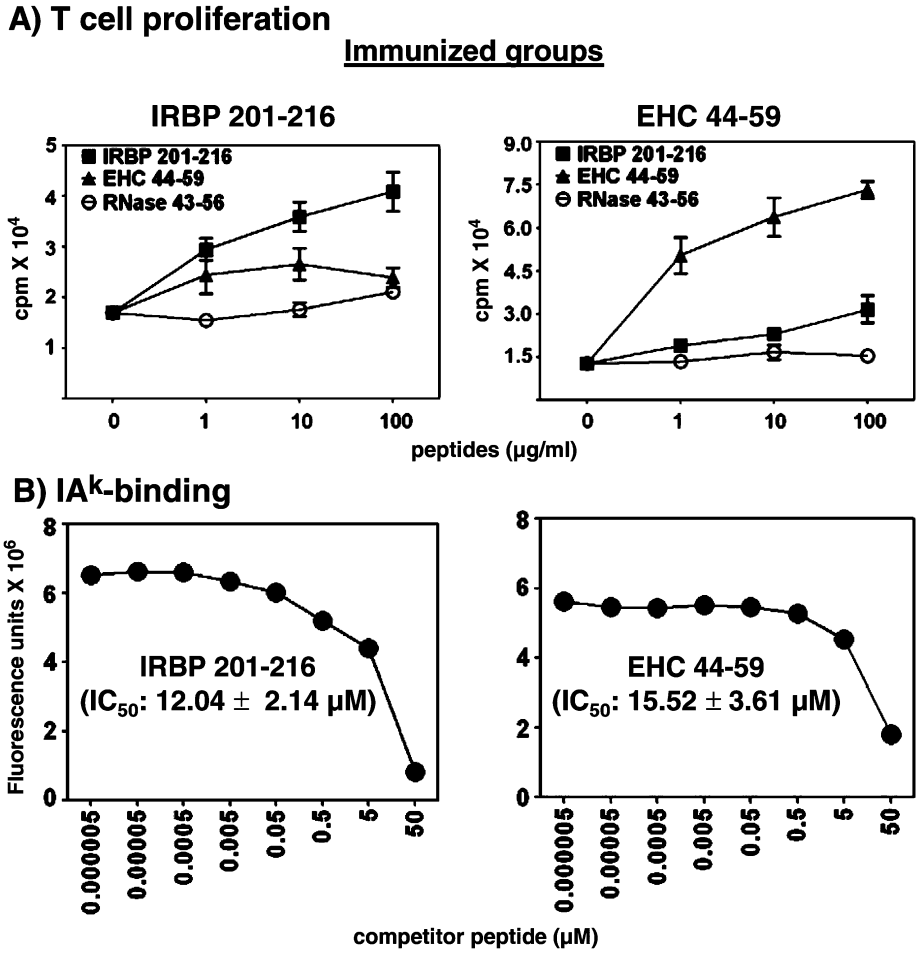

Figure 2. EHC 44–59 induces cross-reactive T cells for IRBP 201–216. A. T cell proliferation. Six- to eight-week-old female A/J mice were immunized with IRBP 201–216 or EHC 44–59 in CFA. After 10 days, mice were sacrificed, the draining LN were harvested and single-cell suspensions were prepared. LNC were stimulated with the indicated peptides for two days followed by pulsing with ^{3}[H] thymidine. Proliferative responses were measured 16 h later as cpm. RNase 43–56, control. Mean ± SEM values obtained from three individual experiments involving 3–4 mice in each are shown. B. IA^k-binding. The reaction mixtures containing thrombin-cleaved IA^k monomers (0.35 µg), competitor peptides (IRBP 201–216 or EHC 44–59: 0.000005 µM to 50 µM) and biotinylated HEL 46–61 (1 µM) were individually prepared and added in duplicate to fluorescence plates coated with anti-IA^k. After washing and addition of europium-labeled SA and DELFIA-enhancer, fluorescence intensities were measured at excitation/emission wavelengths of 340/615 nm, and IC_{50} values were then calculated. Representative data sets (mean ± SEM values) from three to four individual experiments with two replicates in each are shown.

call responses were tested by stimulating the cells with IRBP and its mimicry epitopes (Figure 1). Figure 2A (left panel) shows that IRBP 201–216-sensitized LNC responded to IRBP 201–216 dose dependently as expected, and the response was specific because the cells did not respond to RNase 43–56 (control). Likewise, a proportion of IRBP-reactive cells also reacted to EHC 44–59 (1.6-fold, $p = 0.007$) when compared with the medium controls. Under similar conditions, the T cell responses for other mimics were found to be not more than one-fold (data not shown). Hence, we focused only on EHC 44–59 to determine its ability to induce cross-reactive T cells for IRBP 201–216. As indicated in Figure 2A (right panel), the animals immunized with EHC 44–59 showed strong proliferative responses to EHC 44–59, suggesting that the peptide is immunogenic. Similarly, a fraction of EHC 44–59-sensitized LNC also responded to IRBP 201–216 (2-fold). The data suggest that cross-reactive T cells are induced by each peptide. Finally, we asked whether EHC 44–59 can bind MHC class II/IA^k molecules by establishing IA^k-binding assay (Massilamany et al., 2011b). Using HEL 46–61 as a reference epitope, we ascertained that the IA^k-binding affinities of both IRBP 201–216 and EHC 44–59 were comparable (IC_{50} values: 12.04 ± 2.14 vs. 15.52 ± 3.61 μM; Figure 2B). Thus, we identified EHC 44–59 as a candidate mimicry epitope for IRBP 201–216.

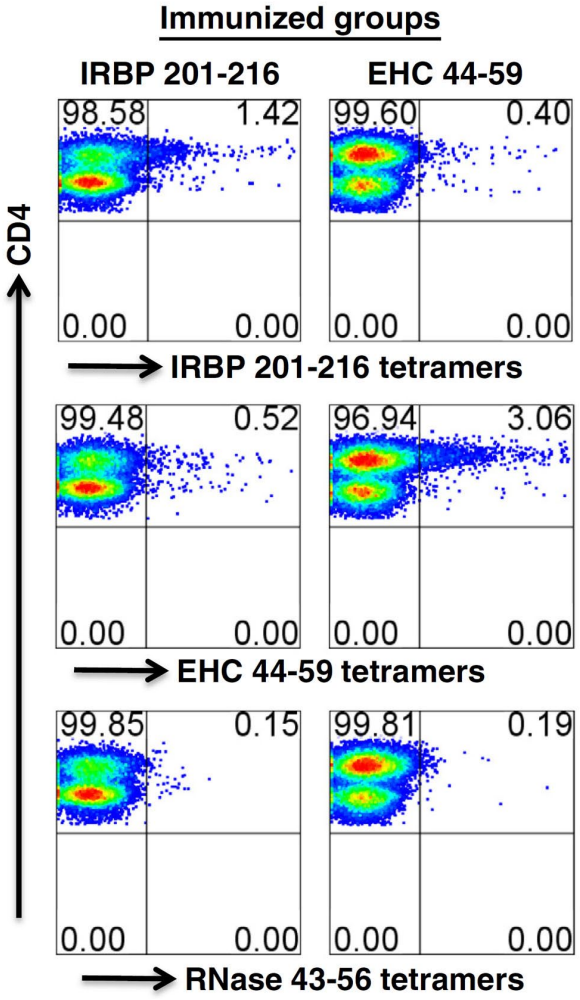

Figure 3. Cross-reactive T cells induced by IRBP 201–216 and EHC 44–59 are antigen specific. Groups of A/J mice were immunized with IRBP 201–216 or EHC 44–59 in CFA. Ten days later, animals were killed and LN were harvested to prepare single cell suspensions. LNC were stimulated with peptides for two days, and the cells were maintained in growth medium containing IL-2 for a week. Viable lymphoblasts were harvested on day 9 poststimulation and stained with IA^k/tetramers, anti-CD4 and 7-AAD. After acquiring the cells by flow cytometry, tet^+ cells were analyzed in the live (7-AAD^-) CD4 subset using FlowJo software. RNase 43–56, control. Representative flow cytometric dot plots from three individual experiments involving 3 to 4 mice in each are shown.

3.3. Cross-reactive T cell responses induced by IRBP 201–216 and EHC 44–59 are antigen-specific

To determine the antigen specificity of CD4 T cell responses induced by IRBP 201–216 and EHC 44–59, we created MHC class II/IA^k tetramers based on a peptide exchange reaction (Massilamany et al., 2011a). Briefly, soluble IA^k monomers containing CLIP 88–102 were initially expressed in the baculovirus, and after cleaving the CLIP peptide, empty IA^k molecules were derived, into which IRBP 201–216, EHC 44–59 or RNase 43–56 (control) peptides were loaded exogenously. The IA^k-peptide complexes were then multimerized to derive tetramers. Antigen-sensitized LNC cultures were derived from mice immunized with IRBP 201–216 or EHC 44–59, and the cells were stained with IA^k/tetramers. As expected, CD4 T cells sensitized with IRBP 201–216 bound to IRBP tetramers (1.42%; Figure 3, top left panel); some also bound to EHC tetramers (0.52%; Figure 3, middle left panel). Similar results were obtained when EHC 44–59-sensitized CD4 T cells were stained with EHC tetramers (3.06%; Figure 3, middle right panel) and IRBP tetramers (0.40%; Figure 3, top right panel). The binding of IRBP 201–216 or EHC 44–59 tetramers was specific, since the staining intensities obtained with the control tetramers (RNase 43–56) were low (~ 0.15%; Figure 3, lower panels). The data suggest that the T cells sensitized with IRBP 201–216 or EHC 44–59 can cross-react with each epitope with specificity.

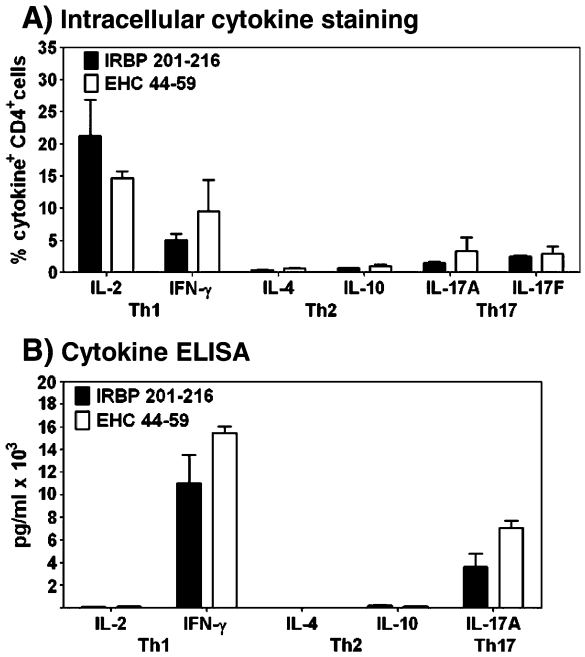

Figure 4. IRBP 201–216 and EHC 44–59 induce identical pattern of cytokines. A. Intracellular cytokine staining. A/J mice were immunized with the indicated peptides in CFA. Ten days later, animals were killed and LN were harvested to prepare single cell suspensions. LNC were stimulated with peptides for two days, and the cells were maintained in growth medium containing IL-2. Viable lymphoblasts were harvested on day 5 poststimulation and stimulated with PMA and ionomycin in the presence of GolgiStop for five hours. After fixation and permeabilization, cells were stained with a panel of antibodies for Th1, Th2 and Th17 cytokines, followed by staining with anti-CD4 and 7-AAD. After acquiring the cells by flow cytometry, cytokine-positive cells were analyzed in the live (7-AAD^-) CD4 subset. Mean ± SEM values derived from three individual experiments involving 3 to 4 mice in each are shown. B. Cytokine ELISA. Culture supernatants harvested from the above cultures on day 2 poststimulation were analyzed by cytokine ELISA. Mean ± SEM values representing three to four individual experiments with two duplicates for each are shown.

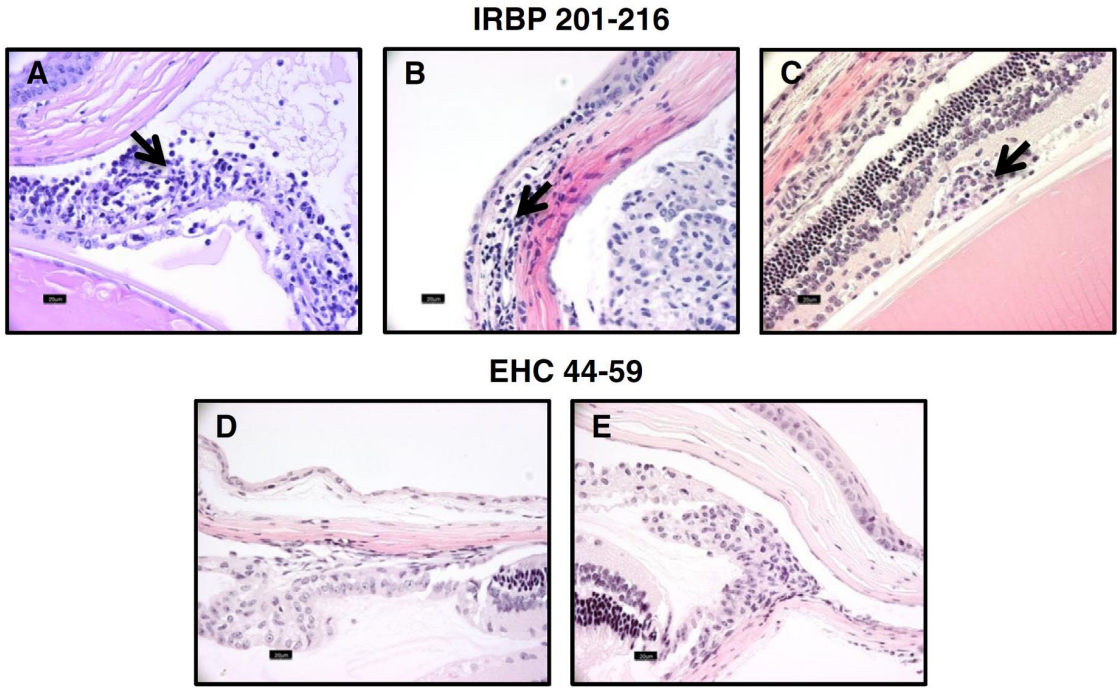

Figure 5. EHC 44–59 failed to induce uveoretinitis in A/J mice. Six- to eight-week-old mice were immunized with IRBP 201–216 or EHC 44–59 (50 μg/mouse) in CFA. PT (100 ng/mouse), was administered intraperitoneally on days 0 and 2 postimmunization. At termination on day 21, the animals were euthanized, and eyes were collected for histological evaluation of inflammation. Note lymphocytic infiltrations in iris (A), corneal–scleral junction (B) and retina (C) in animals immunized with IRBP 201–216 and absence of infiltrates in EHC 44–59-immunized animals (D and E) (arrows: infiltrates). Original magnification, × 40 (bar = 20 μm). Representative data from three to five individual experiments each involving 5 to 9 mice are shown.

3.4. T cells sensitized with IRBP 201–216 or EHC 44–59 produce comparable cytokines

One of the hallmarks of autoreactive T cells is their ability to produce cytokines of Th1 and Th17 phenotypes that favor autoimmunity, including EAU (Damsker et al., 2010; Horai and Caspi, 2011). Therefore, we performed cytokine analysis by intracellular cytokine staining and ELISA for a panel of Th1 (IL-2 and IFN-γ), Th2 (IL-4 and IL-10) and Th17 (IL-17A and IL-17F) cytokines. Enumeration of the frequencies of cytokine-producing CD4 T cells in LNC cultures specific to IRBP 201–216 or EHC 44–59 revealed that the cells capable of producing all of the cytokines tested were present (Figure 4). By analyzing the ratios between the frequencies of Th1-, Th17- and Th2-cytokine producing cells, we noted that a greater percentage of CD4 T cells was positive for Th1 and Th17 than for Th2 cytokines in cultures stimulated with both IRBP 201–216 ($p \leq 0.02$) and EHC 44–59 (Figure 4A). We verified these results by cytokine ELISA using culture supernatants, and the patterns were reproduced for both peptides (Figure 4B; $p \leq 0.03$). The finding that EHC 44–59-responsive cells produced cytokines comparable to those produced by IRBP 201–216-responsive cells raised the possibility that EHC 44–59 may be able to induce EAU in immunized animals.

3.5. EHC 44–59 lacks the ability to induce uveoretinitis

To ascertain the disease-inducing ability of EHC 44–59, we first established a positive control system by optimizing the dose for IRBP 201–216 to induce EAU in immunized animals. Histologically, the infiltrates were predominantly comprised of lymphocytes and a few neutrophils. Doses of IRBP 201–216 up to 50 μg/animal induced comparable histologic EAU, and the inflammatory foci tended to be found more in the corneal–scleral junction, iris and ciliary body than in the choroid, cornea and retina (mean foci ± SEM, 7.75 ± 2.97; Table 2; Figure 5A, B, and C). In contrast, none of the animals immunized with EHC 44–59 showed any evidence of inflammation (Figure 5D and E). This negative disease phenotype could not be altered by increasing PT even up to 1000 ng/animal (Namba et al., 1998; Silver et al., 1999) nor by immunizing the animals twice (Massilamany et al., 2011b; data not shown). Thus, we concluded that EHC 44–59 can generate cross-reactive T cells for IRBP capable of producing Th1 and Th17 cytokines, but it lacks uveitogenicity.

3.6. EHC 44–59 prevents EAU induced with IRBP 201–216

We investigated whether the inability of EHC 44–59 to induce EAU may be due to low frequencies of IRBP-reactive T cells generated in immunized animals. To address this possibility, we first immunized groups of animals with a suboptimal dose (10 μg) of IRBP 201–216; one group of animals was subsequently immunized with EHC 44–59 seven days later, and at termination on day 21, eyes were evaluated for histologic disease. While the animals immunized with IRBP 201–216 alone (5/13 = 38.5%) had inflammatory foci in the eyes [Figure 6A (i) and A (ii)], none of the IRBP 201–216-primed/EHC 44–59-immunized animals (n = 9) showed inflammation [Figure 6A (iii)]. To determine whether this lack of disease was due to

Table 2. Histological EAU induced with IRBP 201–216 and EHC 44–59 in A/J mice.

			Number of foci (mean ± SEM)					Total foci (mean ± SEM)
Peptide	Dose (μg)	Incidence (%)	Corneal–scleral junction	Iris	Cornea	Choroid	Retina	
IRBP 201–216	50	9/20 (45)	2.6 ± 0.89	4.25 ±1.93	0.3 ± 0.22	0.45 ±0.28	0.15 ±0.15	7.75 ±2.97
EHC 44–59	50	0/21 (0)	0	0	0	0	0	0
	100	0/6 (0)	0	0	0	0	0	0

competition between IRBP 201–216 and EHC 44–59 for binding to MHC molecules, we immunized IRBP 201–216-primed animals with a control peptide (RNase 43–56). In this setting, we did observe infiltrates [2/4 = 50%; Figure 6A (iv)], suggesting that competition for MHC between peptides would not have accounted for lack of disease in animals immunized with IRBP and EHC peptides.

We next confirmed that the lack of EAU induction is not due to the absence of IRBP-reactive T cells. As shown in Figure 6B (left panel), the animals primed with IRBP 201–216 showed good proliferative responses to IRBP 201–216 (4.93-fold, p = 6.56E– 06) as compared to those in the medium controls, but the response to EHC 44–59 was low (1.84-fold, p = 0.0033). In contrast, LNC obtained from IRBP 201–216-primed/EHC 44–59-immunized animals responded comparably to both the peptides (IRBP 201–216: 3.4-fold, p = 0.0005; EHC 44–59: 3.6-fold, p = 0.0001; Figure 6B, right panel), indicating that their responses were amplified in response to EHC 44–59-immunization. The data suggest that IRBP-sensitized T cells can expand to a significant proportion in response to EHC 44–59, but the lack of EAU induction in IRBP-primed/EHC-immunized animals raises a question whether EHC 44–59 can behave as a disease-suppressing natural APL.

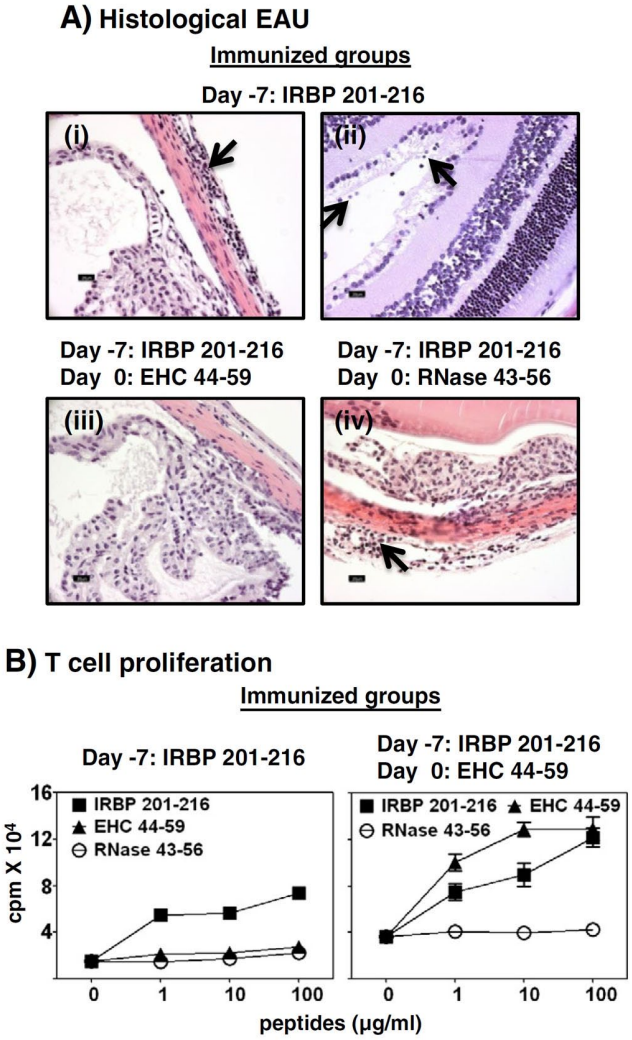

Figure 6. EHC 44–59 prevents development of uveoretinitis induced by IRBP 201–216. A. Histological EAU. Groups of mice were immunized with suboptimal doses of IRBP 201–216 (10 µg/mouse) seven days prior to immunization with or without EHC 44–59 or RNase 43–56 (100 µg/mouse) in CFA, and PT (500 ng/mouse) was administered on day 0 and day 2 after the first immunization. At termination on day 21, eyes were collected for histological evaluation of inflammation. Note scleral and posterior chamber lymphocytic infiltrates in animals immunized with the suboptimal dose of IRBP 201–216 [(i) and (ii)]; normal sclera and ciliary body in animals primed with IRBP 201–216 and later immunized later with EHC 44–59 (iii); and presence of infiltrates in the corneal–scleral junction in animals primed with IRBP 201–216 and subsequently immunized with control peptide (RNase 43–56) (iv). Original magnification, × 40 (bar = 20 µm). Representative data from three individual experiments, each involving 4 to 5 mice, are shown. B. T cell proliferation. LNC harvested from the above groups were stimulated with the indicated peptides for two days followed by pulsing with ^{3}[H] thymidine. Proliferative responses were measured 16 h later as cpm. RNase 43–56, control. Mean ± SEM values derived from representative experiment from three individual experiments, each involving 4 to 5 mice, are shown.

3.7. Altered EHC 44–59 can induce uveoretinitis

To address the possibility that EHC 44–59 can act as an APL, we chose to alter the peptide sequence by substituting the residues within the core region of EHC 44–59, thereby increasing the identity with IRBP 201–216. As indicated in Figure 7A, the region spanning amino acids 45 to 55 contains putative MHC- and TCR-contact residues similar to those in IRBP 201–216. This region of EHC 44–59 is also identical to the same region in IRBP 201–216, except that alanine (Ala) occurs at positions 49 and 52, corresponding to positions 206 and 209 in IRBP 201–216, which contain valine and threonine, respectively. We targeted these residues to generate APLs. In the first APL (EHC 44–59$_{AP1}$), Ala at position 49 was substituted with valine (Val); in the second (EHC 44–59$_{AP2}$), Ala at position 52 was substituted with threonine (Thr); and in the third (EHC 44–59$_{AP3}$), Ala at both positions 49 and 52 were substituted with Val and Thr, respectively (Figure 7A).

We verified the disease-inducing abilities of APLs by immunizing groups of mice (n = 10) and euthanizing animals after three weeks to enucleate the eyes for histological evaluation of EAU. Figure 7B [top panels (i), (ii) and (iii)] shows that the mice immunized with EHC 44–59$_{AP1}$ had inflammatory foci in the sclera, cornea, ciliary body and posterior chamber (3/10 = 30%), and none of the mice immunized with EHC 44–59$_{AP2}$ or EHC 44–59$_{AP3}$ had lesions (Figure 7B, bottom panels). We next examined whether these differential effects of APLs may be due to variations, if any, in the generation of IRBP-reactive T cells in response to APLs. As expected, LNC from mice immunized with IRBP 201–216 responded to IRBP 201–216 with a 3.5-fold enhancement relative to the medium controls, but responses to APLs varied (Figure 7C, upper left panel) in that the response to EHC 44–59$_{AP1}$ was relatively higher (3.3-fold) than responses to the other two APLs. Likewise, by testing the T cell responses in mice immunized with APLs, we noted that LNC from mice immunized with EHC 44–59$_{AP1}$ responded well to both the immunizing peptide and IRBP 201–216 (Figure 7C, upper right panel). Such responses were low in animals immunized with EHC 44–59$_{AP2}$ or EHC 44–59$_{AP3}$ (Figure 7C, bottom panels). Similar differences also were noted with the cytokine analysis, where LNC cultures derived from mice immunized with EHC 44–59$_{AP1}$ contained a higher proportion of IFN-γ-producing Th1 cells than cultures from mice immunized with EHC 44–59$_{AP2}$ (p = 0.045) or EHC 44–59$_{AP3}$ (p = 0.023; Figure 7D). Furthermore, by evaluating the IA^{k}-binding affinities of APLs (Figure 8), we noted that EHC 44–59$_{AP1}$ binds much more strongly to IA^{k} molecules (IC$_{50}$: 4.14 ± 0.28 µM) than do EHC 44–59$_{AP2}$ (IC$_{50}$: 9.35 ± 0.55 µM; p = 0.001) and EHC 44–59$_{AP3}$ (IC$_{50}$: 7.48 ± 0.38 µM; p = 0.002). This may be the reason EHC 44–59$_{AP1}$ has greater immunogenicity and disease-inducing ability than the others. The fact that EHC 44–59 failed to induce EAU on its own and one of its APLs (EHC 44–59$_{AP1}$) induced EAU by preferentially expanding IFN-γ-producing IRBP-reactive T cells further supported the proposal that EHC 44–59 may act as a naturally occurring APL.

4. Discussion

We report here identification of a mimicry epitope from *E. canis* for IRBP 201–216, which is recognized as one of the candidate ocular antigens in EAU pathogenesis (Silver et al., 1995; Namba et al., 1998;

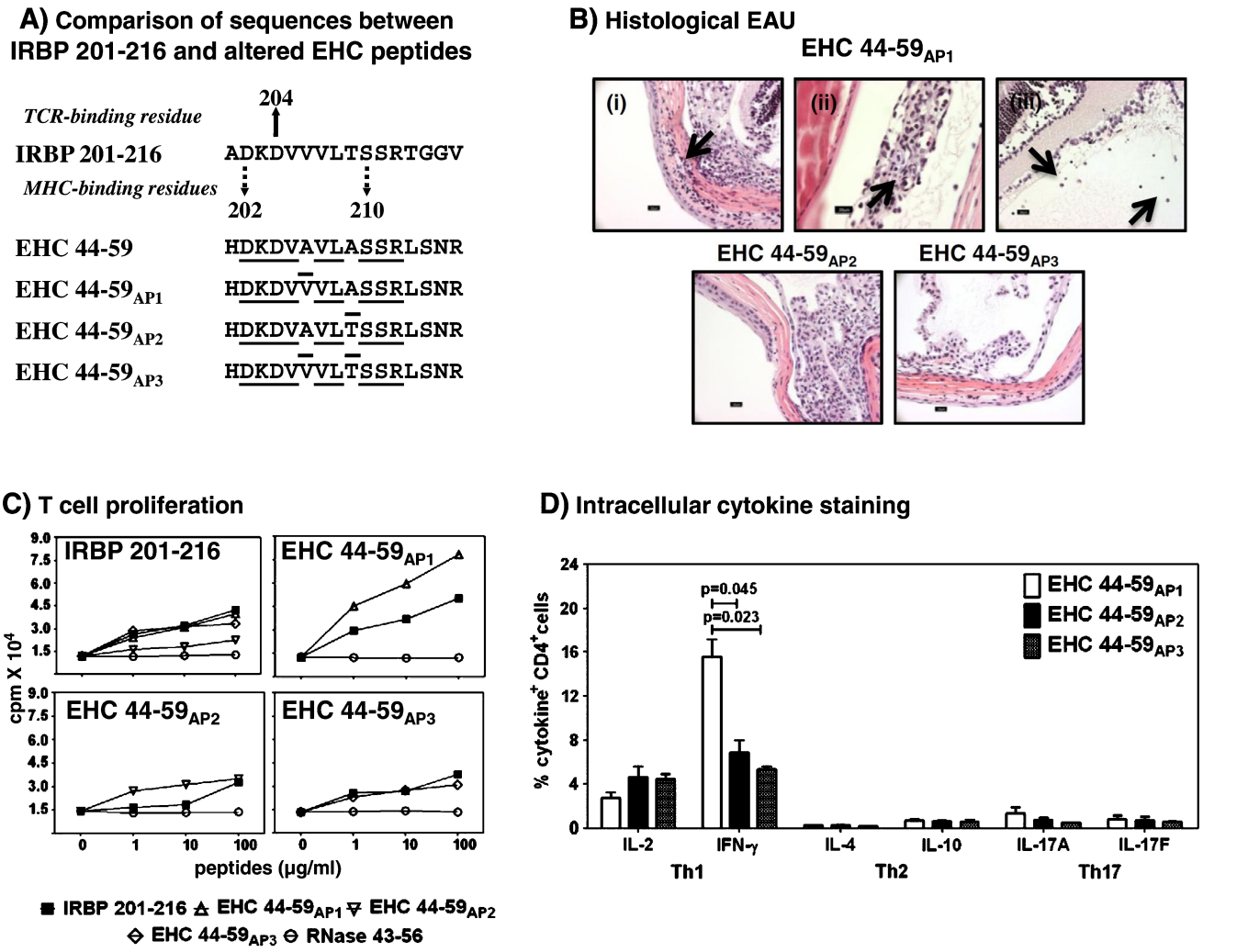

Figure 7. EHC 44–59$_{AP1}$ – but not EHC 44–59$_{AP2}$ and EHC 44–59$_{AP3}$ – induces EAU. A. Comparison of sequences between IRBP 201–216 and altered EHC peptides. Three altered peptides were generated for EHC 44–59, such that Ala at positions 49 and 52 was substituted with Val and Thr, respectively, in the first (EHC 44–59$_{AP1}$) and second peptides (EHC 44–59$_{AP2}$), and both substitutions were made in the third peptide (EHC 44–59$_{AP3}$). Identical residues are underlined, and the substituted residues are overlined. B. Histological EAU. Groups of mice were immunized with the indicated peptides (50 μg/mouse) in CFA, and PT (500 ng/mouse) was administered intraperitoneally on days 0 and 2 postimmunization. At termination on day 21, eyes were enucleated for histological evaluation of inflammation. Note lymphocytic infiltrates at corneal–scleral junctions (i), iris (ii), and posterior chamber (iii) in animals immunized with EHC 44–59$_{AP1}$ (arrows), as opposed to normal sections in animals immunized with EHC 44–59$_{AP2}$ or EHC 44–59$_{AP3}$ (bottom panel). Original magnification, × 40 (bar = 20 μm). Representative data from two individual experiments, each involving five mice, are shown. C. T cell proliferation. LNC generated from the above groups were stimulated with the indicated peptides for two days, and, after pulsing with ^{3}[H] thymidine, proliferative responses were measured as cpm. Data sets from two experiments, each involving 5 to 8 mice, are shown. D. Intracellular cytokine staining. LNC were first stimulated with the indicated peptides for two days in growth medium, and IL-2 was then supplemented. On day 5, viable cells were stimulated with PMA/ionomycin in the presence of GolgiStop for five hours, and, after staining with anti-CD4 and 7-AAD, cells were fixed and permeabilized to stain with cytokine antibodies. Cells were then acquired by flow cytometry, and the percent cytokine^{+} cells were enumerated in the live (7-AAD^{-}) CD4 subset. Mean ± SEM values derived from two individual experiments, each involving 5 mice, are shown.

Cortes et al., 2008; Agarwal et al., 2012). Unexpectedly, instead of functioning as a disease-inducing antigen, the mimicry epitope (EHC 44–59) prevented the disease induced with IRBP 201–216. We provide four lines of evidence to support this finding: 1) EHC 44–59 and IRBP 201–216 contain identical discontinuous stretches of nine residues in which the putative MHC- and TCR-contact residues are localized (Figure 1); 2) T cell responses induced by EHC 44–59 cross-react with IRBP 201–216, and the antigen-sensitized T cells produce predominantly Th1 and Th17 cytokines that promote organ-specific autoimmunity, including EAU (Figure 4; Luger et al., 2008; Yoshimura et al., 2009); 3) the mimicry epitope prevented the development of EAU in animals previously primed with IRBP 201–216, and such an alteration in the disease phenotype was not due to the absence of IRBP-reactive T cells (Figure 6); and 4) finally, one of the altered peptides of the mimicry epitope (EHC 44–59$_{AP1}$) that shows a resemblance to IRBP 201–216 induced EAU through the production of IFN-γ-producing, IRBP-reactive T cells (Figure 7).

Uveitis is a sight-threatening disease that accounts for approximately 10% of severe vision loss (Agarwal et al., 2012), and autoimmune responses have been suspected in the disease mediation (Wildner and Diedrichs-Mohring, 2004; Levy et al., 2011; Agarwal et al., 2012). To delineate the immune events of uveitis, various rodent models of EAU have been developed, and the disease is induced by immunizing the animals with ocular antigens or their peptide fragments (Caspi et al., 1988; Shinohara et al., 1990; Namba et al., 1998; Caspi, 2003; Agarwal et al., 2012). Although it is difficult to recapitulate all events in animal models, histologic features of EAU resemble those of uveitis in humans. Thus, EAU models are commonly employed to study the immune pathogenesis of sight-threatening ocular diseases such as sympathetic ophthalmia, Behcet's disease, birdshot

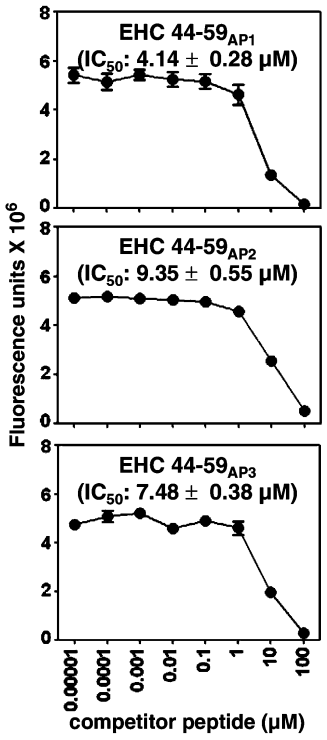

Figure 8. EHC 44–59$_{AP1}$ binds more strongly than EHC 44–59$_{AP2}$ and EHC 44–59$_{AP3}$ to IA^k molecules. The reaction mixtures containing thrombin-cleaved IA^k monomers (0.35 μg) and competitor APLs of EHC 44–59 (0.00001 μM to 100 μM) and biotinylated reference peptide HEL 46–61 (1 μM) were individually prepared and added in duplicate to fluorescence plates coated with anti-IA^k. After washing and addition of europium-labeled SA and DELFIA-enhancer, fluorescence intensities were measured at excitation/emission wavelengths of 340/615 nm, and IC$_{50}$ values were then calculated. Representative data sets (mean ± SEM values) from three individual experiments with two replicates in each are shown.

retinochoroidopathy and Vogt–Koyanagi–Harada syndrome (Agarwal et al., 2012). While rats are susceptible to EAU induced with both soluble antigen (also called arrestin) and IRBP, mice are susceptible to only IRBP, and various uveitogenic epitopes of IRBP have been identified (Caspi et al., 1988; Caspi, 2003; Cortes et al., 2008; Agarwal et al., 2012). One such epitope is IRBP 201–216, which is expected to induce EAU with a relatively higher degree of severity in B10.A mice than in A/J mice (Caspi, 2003), yet both strains possess a similar MHC class II/IA^k allele. However, in our hands, IRBP 201–216, in addition to being less immunogenic, induced EAU with less severity in B10.A mice than in A/J mice (data not shown), leading us to use A/J mice to test the uveitogenicity of mimicry epitopes in our studies.

Generally, exposure to mimicry sequences is expected to lead to induction of pathogenic cross-reactive T cells or autoantibodies (Singh et al., 1990; Shinohara et al., 1991; Rose, 2001, Fujinami et al., 2006; Massilamany et al., 2011b). An exception to this paradigm is the possibility that cross-reactive immune responses may not lead to disease, as shown with a mimic from *Haemophilus influenzae* for myelin proteolipid protein 139–151 (Carrizosa et al., 1998). Alternatively, although less commonly reported, mimicry epitopes can act as APLs by suppressing diseases like experimental autoimmune encephalomyelitis induced with a cognate epitope, myelin basic protein 85–99 (Ruiz et al., 1999; Steinman et al., 2005; Maverakis et al., 2010). Our data with EHC 44–59 agree with the concept that microbial mimics can act as APLs but provide new insights as to their underlying mechanisms.

APLs are believed to act by ablating antigen-specific T cell responses or by deviating cytokine responses from a Th1 (disease-promoting) to a Th2 (disease-suppressing) phenotype and/or promoting the generation of regulatory T cells (Paas-Rozner et al., 2001; Alleva et al., 2002; Aruna et al., 2006). In our studies with EHC 44–59, while generation of antigen (IRBP 201–216)-specific T cell responses was not altered, the EHC-responsive T cells produced both Th1 and Th17 cytokines similar to those produced by IRBP-reactive T cells. On the contrary, production of Th2 cytokines contributed by IL-4 and IL-10 was not elevated. We further ruled out a possibility that differences, if any, in the frequencies of IRBP-reactive T cells could account for lack of disease induced with EHC 44–59 by immunizing the animals primed previously with IRBP 201–216 (Figure 6). In this setting, we noted that T cells specific to both antigens were present, leading to the conclusion that EHC 44–59 did not selectively deplete IRBP-specific cells. However, recent studies indicate that APLs can inhibit T cell activation by affecting phosphorylation of key T cell signaling molecules, such as CD3ζ, CD3ε, Zap-70, src kinases, p56^{lck} and p59^{fyn} (Madrenas et al., 1995; Sloan-Lancaster and Allen, 1996). But we did not investigate these possibilities in our studies.

As additional evidence for a proposal that EHC 44–59 can act as an APL, we altered the peptide sequence to more closely resemble the cognate peptide IRBP 210–216 by changing two Ala residues individually or together. We noted that one peptide (EHC 44–59$_{AP1}$) that contained Val in place of Ala at position 49 was able to induce EAU. EHC 44–59$_{AP3}$ bearing two substitutions at positions 49 and 52 was expected to induce EAU, but this was not the case. Evidently, the amount of IRBP-reactive T cells produced in response to this peptide was also low (Figure 7C, bottom right panel). Further, by cytokine analysis, we noted that the frequencies of IFN-γ-producing cells were elevated only with the disease-inducing peptide EHC 44–59$_{AP1}$ (Figure 7D). Numerous studies indicate that EAU induction requires the mediation of both Th1 and Th17 cells (Xu et al., 1997, 2004; Peng et al., 2007; Luger et al., 2008), but the disease can be induced in C57Bl/6 mice deficient for IFN-γ or IL-17 with deviant or altered disease phenotypes (Caspi et al., 1994; Jones et al., 1997; Luger et al., 2008; Yoshimura et al., 2008). Furthermore, IFN-γ appears to mediate multiple roles (disease-aggravating or disease-protective) in EAU pathogenesis (Jones et al., 1997; Xu et al., 2004; Tang et al., 2007). Whether such differential effects are dose dependent is not known. Since EHC 44–59$_{AP1}$ induced higher frequencies of IFN-γ-producing IRBP-reactive T cells than two other altered peptides (EHC 44–59$_{AP2}$ and EHC 44–59$_{AP3}$), our data suggest that IFN-γ-producing cells may have led to the disease mediation.

In summary, we have provided evidence that a mimicry epitope derived from *E. canis* can act as a naturally occurring APL by suppressing the disease induced with IRBP 201–216 without altering IRBP-specific T cell responses. To induce cross-reactive immune responses for microbes carrying mimicry epitopes, humans need not be natural hosts. Conversely, the natural pathogens of humans carrying the mimicry epitopes can induce inflammation by generating cross-reactive immune responses, but such responses can be detrimental to the survival of parasites. It may be that, evolutionarily, coexistence of parasites with hosts may promote acquisition of the host's genetic material, and introduction of mutations under selection pressure may favor attenuation of the host's immune response, leading to their survival.

References

Agarwal, R.K., Silver, P.B., Caspi, R.R., 2012. Rodent models of experimental autoimmune uveitis. Methods Mol. Biol. 900, 443–469.

Alleva, D.G., Gaur, A., Jin, L., Wegmann, D., Gottlieb, P.A., Pahuja, A., Johnson, E.B., Motheral, T., Putnam, A., Crowe, P.D., Ling, N., Boehme, S.A., Conlon, P.J., 2002. Immunological characterization and therapeutic activity of an altered-peptide ligand, NBI- 6024, based on the immunodominant type 1 diabetes autoantigen insulin B-chain (9–23) peptide. Diabetes 51, 2126–2134.

Anderson, A.C., Nicholson, L.B., Legge, K.L., Turchin, V., Zaghouani, H., Kuchroo, V.K., 2000. High frequency of autoreactive myelin proteolipid protein-specific T cells in the periphery of naive mice: mechanisms of selection of the self-reactive repertoire. J. Exp. Med. 191, 761–770.

Aruna, B.V., Sela, M., Mozes, E., 2006. Down-regulation of T cell responses to AChR and reversal of EAMG manifestations in mice by a dual altered peptide ligand via induction of CD4+ CD25+ regulatory cells. J. Neuroimmunol. 177, 63–75.

Benhar, I., London, A., Schwartz, M., 2012. The privileged immunity of immune privileged organs: the case of the eye. Front. Immunol. 3, 296.

Carrizosa, A.M., Nicholson, L.B., Farzan, M., Southwood, S., Sette, A., Sobel, R.A., Kuchroo, V.K., 1998. Expansion by self antigen is necessary for the induction of experimental autoimmune encephalomyelitis by T cells primed with a cross-reactive environmental antigen. J. Immunol. 161, 3307–3314.

Caspi, R.R., 2003. Experimental autoimmune uveoretinitis in the rat and mouse. Curr. Protoc. Immunol. http://dx.doi.org/10.1002/0471142735.im1506s53 (Chapter 15, Unit 15.6).

Caspi, R.R., 2006. Ocular autoimmunity: the price of privilege? Immunol. Rev. 213, 23–35.

Caspi, R.R., Roberge, F.G., Chan, C.C., Wiggert, B., Chader, G.J., Rozenszajn, L.A., Lando, Z., Nussenblatt, R.B., 1988. A new model of autoimmune disease. Experimental autoimmune uveoretinitis induced in mice with two different retinal antigens. J. Immunol. 140, 1490–1495.

Caspi, R.R., Chan, C.C., Grubbs, B.G., Silver, P.B., Wiggert, B., Parsa, C.F., Bahmanyar, S., Billiau, A., Heremans, H., 1994. Endogenous systemic IFN-gamma has a protective role against ocular autoimmunity in mice. J. Immunol. 152, 890–899.

Charukamnoetkanok, P., Fukushima, A., Whitcup, S.M., Gery, I., Egwuagu, C.E., 1998. Expression of ocular autoantigens in the mouse thymus. Curr. Eye Res. 17, 788–792.

Cortes, L.M., Mattapallil,M.J., Silver, P.B., Donoso, L.A., Liou, G.I., Zhu, W., Chan, C.C., Caspi, R.R., 2008. Repertoire analysis and new pathogenic epitopes of IRBP in C57BL/6 (H-2b) and B10.RIII (H-2r) mice. Invest. Ophthalmol. Vis. Sci. 49, 1946–1956.

Cousins, S.W., McCabe, M.M., Danielpour, D., Streilein, J.W., 1991. Identification of transforming growth factor-beta as an immunosuppressive factor in aqueous humor. Invest. Ophthalmol. Vis. Sci. 32, 2201–2211.

Damsker, J.M., Hansen, A.M., Caspi, R.R., 2010. Th1 and Th17 cells: adversaries and collaborators. Ann. N. Y. Acad. Sci. 1183, 211–221.

Day, C.L., Seth, N.P., Lucas, M., Appel, H., Gauthier, L., Lauer, G.M., Robbins, G.K., Szczepiorkowski, Z.M., Casson, D.R., Chung, R.T., Bell, S., Harcourt, G., Walker, B.D., Klenerman, P., Wucherpfennig, K.W., 2003. Ex vivo analysis of human memory CD4 T cells specific for hepatitis C virus using MHC class II tetramers. J. Clin. Invest. 112, 831–842.

Forrester, J.V., Xu, H., 2012. Good news–bad news: the Yin and Yang of immune privilege in the eye. Front. Immunol. 3, 1–18.

Fujinami, R.S., Oldstone, M.B., 1985. Amino acid homology between the encephalitogenic site of myelin basic protein and virus: mechanism for autoimmunity. Science 230, 1043–1045.

Fujinami, R.S., von Herrath, M.G., Christen, U., Whitton, J.L., 2006. Molecular mimicry, bystander activation, or viral persistence: infections and autoimmune disease. Clin. Microbiol. Rev. 19, 80–94.

Gangaplara, A., Massilamany, C., Brown, D.M., Delhon, G., Pattnaik, A.K., Chapman, N., Rose, N., Steffen, D., Reddy, J., 2012. Coxsackievirus B3 infection leads to the generation of cardiac myosin heavy chain-alpha-reactive CD4 T cells in A/J mice. Clin. Immunol. 144, 237–249.

Hamrah, P., Dana, M.R., 2007. Corneal antigen-presenting cells. Chem. Immunol. Allergy 92, 58–70.

Hausmann, D.H., Yu, B., Hausmann, S., Wucherpfennig, K.W., 1999. pH-dependent peptide binding properties of the type I diabetes-associated I-Ag7 molecule: rapid release of CLIP at an endosomal pH. J. Exp. Med. 189, 1723–1734.

Horai, R., Caspi, R.R., 2011. Cytokines in autoimmune uveitis. J. Interferon Cytokine Res. 31, 733–744.

Jones, L.S., Rizzo, L.V., Agarwal, R.K., Tarrant, T.K., Chan, C.C., Wiggert, B., Caspi, R.R., 1997. IFN-gamma-deficient mice develop experimental autoimmune uveitis in the context of a deviant effector response. J. Immunol. 158, 5997–6005.

Klein, L., Klugmann, M., Nave, K.A., Tuohy, V.K., Kyewski, B., 2000. Shaping of the autoreactive T-cell repertoire by a splice variant of self protein expressed in thymic epithelial cells. Nat. Med. 6, 56–61.

Levy, R.A., de Andrade, F.A., Foeldvari, I., 2011. Cutting-edge issues in autoimmune uveitis. Clin. Rev. Allergy Immunol. 41, 214–223.

Luger, D., Silver, P.B., Tang, J., Cua, D., Chen, Z., Iwakura, Y., Bowman, E.P., Sgambellone, N.M., Chan, C.C., Caspi, R.R., 2008. Either a Th17 or a Th1 effector response can drive autoimmunity: conditions of disease induction affect dominant effector category. J. Exp. Med. 205, 799–810.

Madrenas, J., Wange, R.L., Wang, J.L., Isakov, N., Samelson, L.E., Germain, R.N., 1995. Zeta phosphorylation without ZAP-70 activation induced by TCR antagonists or partial agonists. Science 267, 515–518.

Massilamany, C., Steffen, D., Reddy, J., 2009. An epitope from Acanthamoeba castellanii that cross-react with proteolipid protein 139–151-reactive T cells induces autoimmune encephalomyelitis in SJL mice. J. Neuroimmunol. 219, 17–24.

Massilamany, C., Thulasingam, S., Steffen, D., Reddy, J., 2010. Gender differences in CNS autoimmunity induced by mimicry epitope for PLP 139–151 in SJL mice. J. Neuroimmunol. 230, 95–104.

Massilamany, C., Gangaplara, A., Chapman, N., Rose, N., Reddy, J., 2011a. Detection of cardiac myosin heavy chain-alpha-specific CD4 cells by using MHC class II/IA(k) tetramers in A/J mice. J. Immunol. Methods 372, 107–118.

Massilamany, C., Gangaplara, A., Steffen, D., Reddy, J., 2011b. Identification of novel mimicry epitopes for cardiacmyosin heavy chain-alpha that induce autoimmunemyocarditis in A/J mice. Cell. Immunol. 271, 438–449.

Maverakis, E., Menezes, J.S., Ametani, A., Han, M., Stevens, D.B., He, Y., Wang, Y., Ono, Y., Miyamura, Y., Lam, K.S., Ward, E.S., Sercarz, E.E., 2010. Molecular mimics can induce a nonautoaggressive repertoire that preempts induction of autoimmunity. Proc. Natl. Acad. Sci. U. S. A. 107, 2550–2555.

Miller, S.D., Vanderlugt, C.L., Begolka,W.S., Pao,W., Neville, K.L., Yauch, R.L., Kim, B.S., 1997a. Epitope spreading leads to myelin-specific autoimmune responses in SJL mice chronically infected with Theiler's virus. J. Neurovirol. 3 (Suppl. 1), S62–S65.

Miller, S.D., Vanderlugt, C.L., Begolka, W.S., Pao,W., Yauch, R.L., Neville, K.L., Katz-Levy, Y., Carrizosa, A., Kim, B.S., 1997b. Persistent infection with Theiler's virus leads to CNS autoimmunity via epitope spreading. Nat. Med. 3, 1133–1136.

Namba, K., Ogasawara, K., Kitaichi, N., Matsuki, N., Takahashi, A., Sasamoto, Y., Kotake, S., Matsuda, H., Iwabuchi, K., Ohno, S., Onoe, K., 1998. Identification of a peptide inducing experimental autoimmune uveoretinitis (EAU) in H-2Ak-carrying mice. Clin. Exp. Immunol. 111, 442–449.

Oldstone, M.B., 2005. Molecular mimicry, microbial infection, and autoimmune disease: evolution of the concept. Curr. Top. Microbiol. Immunol. 296, 1–17.

Olson, J.K., Eagar, T.N., Miller, S.D., 2002. Functional activation of myelin-specific T cells by virus-induced molecular mimicry. J. Immunol. 169, 2719–2726.

Paas-Rozner, M., Sela, M., Mozes, E., 2001. The nature of the active suppression of responses associated with experimental autoimmune myasthenia gravis by a dual altered peptide ligand administered by different routes. Proc. Natl. Acad. Sci. U. S. A. 98, 12642–12647.

Peng, Y., Han, G., Shao, H.,Wang, Y., Kaplan, H.J., Sun, D., 2007. Characterization of IL-17+ interphotoreceptor retinoid-binding protein-specific T cells in experimental autoimmune uveitis. Invest. Ophthalmol. Vis. Sci. 48, 4153–4161.

Rose, N.R., 2001. Infection, mimics, and autoimmune disease. J. Clin. Invest. 107, 943–944.

Ruiz, P.J., Garren, H., Hirschberg, D.L., Langer-Gould, A.M., Levite, M., Karpuj, M.V., Southwood, S., Sette, A., Conlon, P., Steinman, L., 1999. Microbial epitopes act as altered peptide ligands to prevent experimental autoimmune encephalomyelitis. J. Exp. Med. 189, 1275–1284.

Shinohara, T., Singh, V.K., Tsuda, M., Yamaki, K., Abe, T., Suzuki, S., 1990. S-antigen: from gene to autoimmune uveitis. Exp. Eye Res. 50, 751–757.

Shinohara, T., Singh, V.K., Yamaki, K., Abe, T., Tsuda,M., Suzuki, S., 1991. S-antigen: molecular mimicry may play a role in autoimmune uveitis. Prog. Clin. Biol. Res. 362, 163–190.

Silver, P.B., Rizzo, L.V., Chan, C.C., Donoso, L.A., Wiggert, B., Caspi, R.R., 1995. Identification of a major pathogenic epitope in the human IRBP molecule recognized by mice of the H-2r haplotype. Invest. Ophthalmol. Vis. Sci. 36, 946–954.

Silver, P.B., Chan, C.C., Wiggert, B., Caspi, R.R., 1999. The requirement for pertussis to induce EAU is strain-dependent: B10.RIII, but not B10.A mice, develop EAU and Th1 responses to IRBP without pertussis treatment. Invest. Ophthalmol. Vis. Sci. 40, 2898–2905.

Singh, V.K., Kalra, H.K., Yamaki, K., Abe, T., Donoso, L.A., Shinohara, T., 1990. Molecular mimicry between a uveitopathogenic site of S-antigen and viral peptides. Induction of experimental autoimmune uveitis in Lewis rats. J. Immunol. 144, 1282–1287.

Sloan-Lancaster, J., Allen, P.M., 1996. Altered peptide ligand-induced partial T cell activation: molecular mechanisms and role in T cell biology. Annu. Rev. Immunol. 14, 1–27.

Steinman, L., Utz, P.J., Robinson, W.H., 2005. Suppression of autoimmunity via microbial mimics of altered peptide ligands. Curr. Top. Microbiol. Immunol. 296, 55–63. Streilein, J.W., Masli, S., Takeuchi, M., Kezuka, T., 2002. The eye's view of antigen presentation. Hum. Immunol. 63, 435–443.

Takase, H., Yu, C.R., Mahdi, R.M., Douek, D.C., Dirusso, G.B., Midgley, F.M., Dogra, R., Allende, G., Rosenkranz, E., Pugliese, A., Egwuagu, C.E., Gery, I., 2005. Thymic expression of peripheral tissue antigens in humans: a remarkable variability among individuals. Int. Immunol. 17, 1131–1140.

Tang, J., Zhu, W., Silver, P.B., Su, S.B., Chan, C.C., Caspi, R.R., 2007. Autoimmune uveitis elicited with antigen-pulsed dendritic cells has a distinct clinical signature and is driven by unique effector mechanisms: initial encounter with autoantigen defines disease phenotype. J. Immunol. 178, 5578–5587.

Vallochi, A.L., Commodaro, A.G., Schwartzman, J.P., Belfort Jr., R., Rizzo, L.V., 2007. The role of cytokines in the regulation of ocular autoimmune inflammation. Cytokine Growth Factor Rev. 18, 135–141.

Wildner, G., Diedrichs-Mohring, M., 2004. Autoimmune uveitis and antigenic mimicry of environmental antigens. Autoimmun. Rev. 3, 383–387.

Xu, H., Rizzo, L.V., Silver, P.B., Caspi, R.R., 1997. Uveitogenicity is associated with a Th1-like lymphokine profile: cytokine-dependent modulation of early and committed effector T cells in experimental autoimmune uveitis. Cell. Immunol. 178, 69–78.

Xu, H., Manivannan, A., Jiang, H.R., Liversidge, J., Sharp, P.F., Forrester, J.V., Crane, I.J., 2004. Recruitment of IFN-gamma-producing (Th1-like) cells into the inflamed retina in vivo is preferentially regulated by P-selectin glycoprotein ligand 1:P/E-selectin interactions. J. Immunol. 172, 3215–3224.

Yoshimura, T., Sonoda, K.H.,Miyazaki, Y., Iwakura, Y., Ishibashi, T., Yoshimura, A., Yoshida, H., 2008. Differential roles for IFN-gamma and IL-17 in experimental autoimmune uveoretinitis. Int. Immunol. 20, 209–214.

Yoshimura, T., Sonoda, K.H., Ohguro, N., Ohsugi, Y., Ishibashi, T., Cua, D.J., Kobayashi, T., Yoshida, H., Yoshimura, A., 2009. Involvement of Th17 cells and the effect of anti- IL-6 therapy in autoimmune uveitis. Rheumatology (Oxford) 48, 347–354.